SUPPLEMENT

ANTHROPOGENIC CONTRIBUTIONS TO THE 2018 EXTREME FLOODING OVER THE UPPER YELLOW RIVER BASIN IN CHINA

Peng Ji, Xing Yuan, Yang Jiao, Chunqing Wang, Shuai Han, and Chunxiang Shi

This document is a supplement to "Anthropogenic Contributions to the 2018 Extreme Flooding over the Upper Yellow River Basin in China," by Peng Ji, Xing Yuan, Yang Jiao, Chunqing Wang, Shuai Han, and Chunxiang Shi (*Bull. Amer. Meteor. Soc.*, **101**, S89–S94) • ©2020 American Meteorological Society • *Corresponding author:* Xing Yuan, xyuan@nuist.edu.cn • DOI:10.1175/BAMS-D-19-0105.2

BIAS CORRECTION. The cumulative distribution function (CDF) matching bias correction method, which is widely used both in hydrological modeling (Sharma et al. 2007; Terink et al. 2010) and extreme streamflow attributions (Ji and Yuan 2018; Li et al. 2010; Roudier et al. 2016), is used in this research. First, daily precipitation and temperature from CMIP5 models were regridded to 10-km resolution by using conservation and bilinear interpolation methods respectively. Second, CDFs for observation and CMIP5 ALL simulations were calculated. Third, CMIP5 ALL simulations were corrected to the observations by matching their ranks in the CDFs. Finally, the CMIP5 NAT simulations were corrected by using CDFs of ALL simulations to preserve the difference between NAT and ALL scenarios (Fig. ES1c). The bias correction was done at each 10-km-resolution grid for both precipitation and temperature, which means systematic bias caused by differences in topography can be removed. After bias correction, CDFs of monthly ALL simulations are the same as observation while differences between ALL and NAT are generally preserved (Fig. ES1c). Moreover, the bias-corrected ALL simulations can reasonably capture the distributions of daily precipitation (Fig. ES1d) and extremes (Fig. ES1e). The difference of extreme precipitation between ALL and NAT can also be generally preserved because the CDF matching keeps the rank of precipitation values (Fig. ES1f).

LAND SURFACE MODEL EVALUATION. LUCC_CSSPv2 was first evaluated by using the monthly naturalized streamflow. Figure ES1g shows that LUCC_CSSPv2 well captures monthly naturalized streamflow variations during 1987–2010, with Nash–Sutcliffe efficiency and correlation coefficient being 0.87 and 0.95, respectively. Second, daily streamflow simulation was evaluated by using observed daily streamflow during 1971–86, assuming that observed streamflow differs little from the naturalized streamflow when influences of reservoirs are relatively small during this period. Results show that LUCC_CSSPv2 simulates daily streamflow well during 1971–86 (Fig. ES1h), with the Nash–Sutcliffe efficiency and correlation coefficient being 0.70 and 0.88 respectively. The relative biases for daily streamflow and its annual maximum are –3% and –2% respectively, suggesting the good performance of LUCC_CSSPv2.

CONTRIBUTIONS OF DIFFERENT ANTHROPOGENIC FACTORS. The observed probability of extreme flooding can be written as $P_{OBS} = P_{NAT} + \Delta P_{ANT} + \Delta P_{LUCC} + \Delta P_{RES}$, where the P_{NAT} is probability of extreme flooding when the climate internal variability and natural climate change are considered, while ΔP_{ANT}, ΔP_{LUCC}, and ΔP_{RES} are the influences of anthropogenic climate change (ANT), land use/cover change (LUCC), and reservoir operation (RES). According to the experiments in this study, they were calculated as

$$\begin{cases} \Delta P_{\mathrm{ANT}} = P_{\mathrm{FIXED\_CSSPv2}} - P_{\mathrm{NAT}} \\ \Delta P_{\mathrm{LUCC}} = P_{\mathrm{LUCC\_CSSPv2}} - P_{\mathrm{FIXED\_CSSPv2}} \\ \Delta P_{\mathrm{RES}} = P_{\mathrm{OBS}} - P_{\mathrm{LUCC\_CSSPv2}} \end{cases}. \tag{ES1}$$

To make the results comparable, we use the natural condition (P_{ANT}) as the reference. Thus the risk ratio (RR) of one anthropogenic factor can be written as

$$\begin{cases} \mathrm{RR}_{\mathrm{ANT}} = \left(P_{\mathrm{NAT}} + \Delta P_{\mathrm{ANT}}\right)/P_{\mathrm{NAT}} \\ \mathrm{RR}_{\mathrm{LUCC}} = \left(P_{\mathrm{NAT}} + \Delta P_{\mathrm{LUCC}}\right)/P_{\mathrm{NAT}} \\ \mathrm{RR}_{\mathrm{RES}} = \left(P_{\mathrm{NAT}} + \Delta P_{\mathrm{RES}}\right)/P_{\mathrm{NAT}} \end{cases}. \tag{ES2}$$

Substituting Eq. (ES1) into Eq. (ES2), we can get

$$\begin{cases} \mathrm{RR}_{\mathrm{ANT}} = P_{\mathrm{FIXED\_CSSPv2}}/P_{\mathrm{NAT}} \\ \mathrm{RR}_{\mathrm{LUCC}} = \left[P_{\mathrm{NAT}} + \left(P_{\mathrm{LUCC\_CSSPv2}} - P_{\mathrm{FIXED\_CSSPv2}}\right)\right]/P_{\mathrm{NAT}} \\ \mathrm{RR}_{\mathrm{RES}} = \left[P_{\mathrm{NAT}} + \left(P_{\mathrm{OBS}} - P_{\mathrm{LUCC\_CSSPv2}}\right)\right]/P_{\mathrm{NAT}} \end{cases}. \tag{ES3}$$

The contribution of a factor in decreasing the likelihood of extreme flooding (CTR) can be then estimated as

$$\begin{cases} \mathrm{CTR}_{\mathrm{ANT}} = 1 - \mathrm{RR}_{\mathrm{ANT}} = \left(P_{\mathrm{NAT}} - P_{\mathrm{FIXED\_CSSPv2}}\right)/P_{\mathrm{NAT}} = \mathrm{RR}_{\mathrm{NAT}} - \mathrm{RR}_{\mathrm{FIXED\_CSSPv2}} \\ \mathrm{CTR}_{\mathrm{LUCC}} = 1 - \mathrm{RR}_{\mathrm{LUCC}} = \left(P_{\mathrm{FIXED\_CSSPv2}} - P_{\mathrm{LUCC\_CSSPv2}}\right)/P_{\mathrm{NAT}} = \mathrm{RR}_{\mathrm{FIXED\_CSSPv2}} - \mathrm{RR}_{\mathrm{LUCC\_CSSPv2}} \\ \mathrm{CTR}_{\mathrm{RES}} = 1 - \mathrm{RR}_{\mathrm{RES}} = \left(P_{\mathrm{LUCC\_CSSPv2}} - P_{\mathrm{OBS}}\right)/P_{\mathrm{NAT}} = \mathrm{RR}_{\mathrm{LUCC\_CSSPv2}} - \mathrm{RR}_{\mathrm{OBS}} \end{cases} \tag{ES4}$$

Now we can directly use the risk ratio of different experiments to estimate the contributions of three factors. The nominator of equation (ES4) is how much impact a factor would have on the likelihood of an extreme event while the denominator is to rescale this impact to the likelihood in natural world.

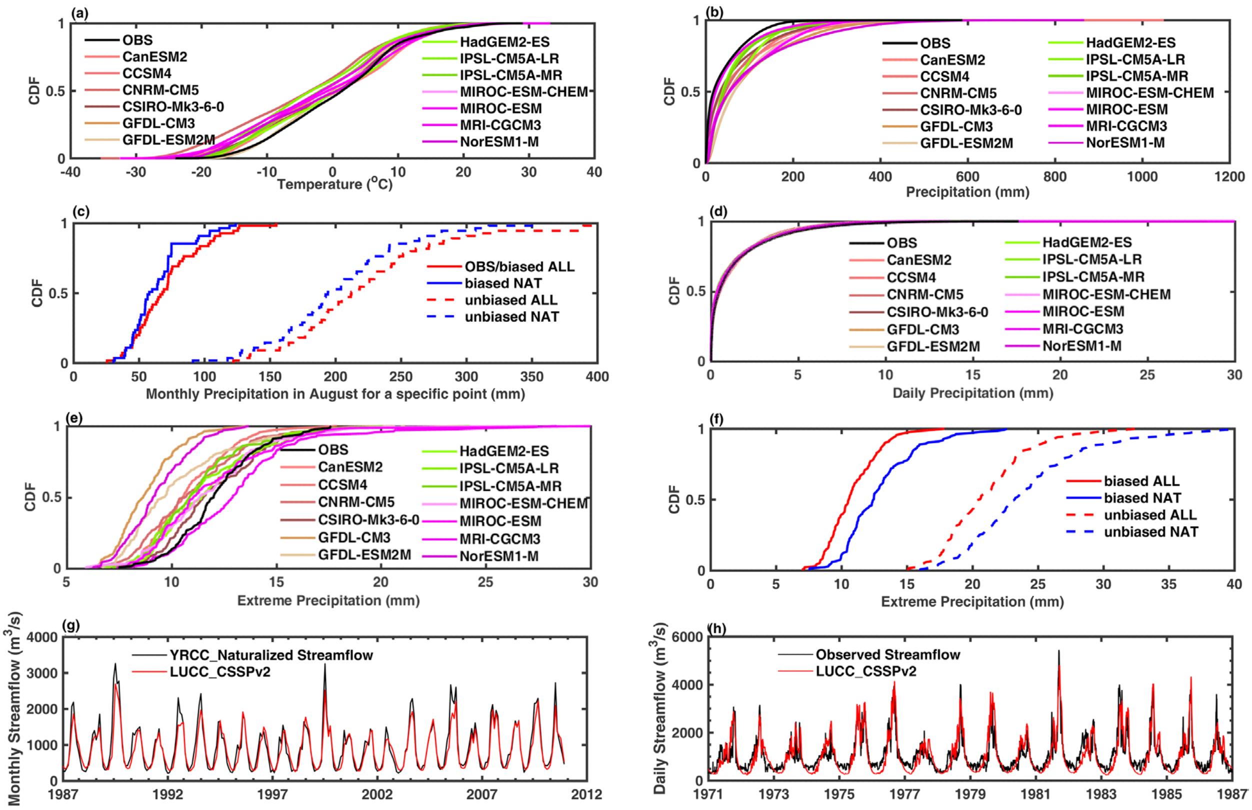

Fig. ES1. (a) Cumulative distribution functions (CDFs) of observed and CMIP5 model simulated monthly temperature over the upper Yellow River basin (UYRB) during 1961–2005. Monthly data of each grid in UYRB were used to estimate the CDFs. (b) As in (a), but for monthly precipitation. (c) Example of CDF bias correction for monthly precipitation simulated by CanESM2. (d),(e) As in (b), but for daily precipitation and extreme precipitation (>99% percentile) respectively. (f) Comparison between CDFs of extreme precipitation in ALL and NAT scenarios simulated by CanESM2 before and after bias correction. (g) Comparison between naturalized monthly streamflow (YRCC_Naturalized Streamflow) and CSSPv2 simulated streamflow with land cover change (LUCC_CSSPv2). (h) Comparison between observed daily streamflow and simulations in LUCC_CSSPv2.

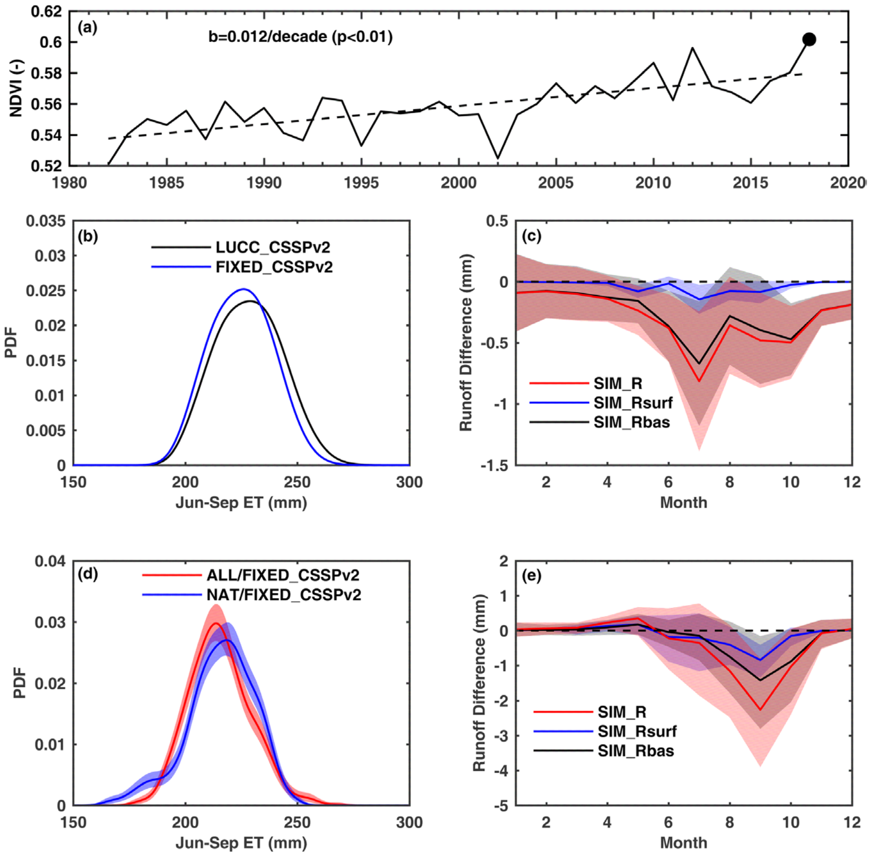

Fig. ES2. (a) June–September mean Normalized Difference Vegetation Index (NDVI) averaged over the upper Yellow River basin during 1982–2018 (solid line) and its linear trend (dashed line). (b) Probability density functions (PDFs) of June–September mean evapotranspiration simulated by the CSSPv2 model with (LUCC_CSSPv2) or without (FIXED_CSSPv2) land cover changes. (c) Impacts of land cover change on simulated seasonal cycles of total runoff (SIM_R), surface runoff (SIM_Rsurf), and subsurface runoff (SIM_Rbas) averaged over the upper Yellow River basin. (d) As in (b), but for simulations driven by CMIP5 outputs. (e) As in (c), but for impacts of anthropogenic climate change. Shaded areas in (c)–(e) are 95% confidence intervals.

Table ES1. Details for CMIP5 model simulations used in this study. Both the ALL and NAT simulations during 1951–2005 from only one pair of realization (r1i1p1) were used to assure an equal weight for different CMIP5 models (Wang et al. 2019). The ALL simulations were forced by both anthropogenic (greenhouse gases, anthropogenic aerosols, etc.) and natural (solar and volcanic activities) external factors, while NAT simulations were forced by natural factors only.

No.	Models	Horizontal resolution (lon × lat grid points)
1	CanESM2	128 × 64
2	CCSM4	288 × 192
3	CNRM-CM5	256 × 128
4	CSIRO-Mk3.6.0	192 × 96
5	GFDL CM3	144 × 90
6	GFDL-ESM2M	144 × 90
7	HadGEM2-ES	192 × 145
8	IPSL-CM5A-LR	96 × 96
9	IPSL-CM5A-MR	144 × 143
10	MIROC-ESM	128 × 64
11	MIROC-ESM-CHEM	128 × 64
12	MRI-CGCM3	320 × 160
13	NorESM1-M	144 × 96